Biomaterials 30 (2009) 1962–1970

Contents lists available at ScienceDirect

Biomaterials

journal homepage: www.elsevier.com/locate/biomaterials

MRI-visible polymeric vector bearing CD3 single chain antibody for gene delivery to T cells for immunosuppression

Chen Guihua[a,*,1], Chen Wenjie[a,1], Wu Zhuang[a,1], Yuan Renxu[b,1], Li Hua[a], Gao Jinming[c], Shuai Xintao[b,**]

[a] Liver Transplantation Center, The Third Affiliated Hospital, Sun Yat-Sen University, Guangzhou 510630, China
[b] Center of Biomedical Engineering, School of Chemistry and Chemical Engineering, Sun Yat-Sen University, Guangzhou 510275, China
[c] Department of Pharmacology, Simmons Comprehensive Cancer Center, University of Texas Southwestern Medical Center at Dallas, Dallas, TX, USA

ARTICLE INFO

Article history:
Received 2 November 2008
Accepted 15 December 2008
Available online 21 January 2009

Keywords:
Immunosuppression
Targeted gene delivery
T cell anergy
Nonviral vector
Magnetic resonance imaging

ABSTRACT

Gene therapy mediated by nonviral vectors provides great advantages over conventional drug therapy in inducing immunosuppression after organ transplantation, yet it was rarely reported because T cells are normally difficult to transfect. In this paper, a nonviral vector that effectively transports genes into T cells is developed by attaching a T cell specific ligand, the CD3 single chain antibody ($scAb_{CD3}$), to the distal ends of poly(ethylene glycol)-grafted polyethylenimine ($scAb_{CD3}$-PEG-*g*-PEI). This polymer was first complexed with superparamagnetic iron oxide nanoparticles (SPIONs) and was then used to condense plasmid DNA into nanoparticles with an ideally small size and low cytotoxicity. Based on a reporter gene assay, targeting ligand functionalization of the delivery agent leads to 16 fold of enhancement in the gene transfection level in HB8521 cells, a rat T lymphocyte line. This targeting event in cell culture was successfully imaged by MRI scan. Inspiringly, delivery of a therapeutic gene DGKα with our MRI-visible delivery agent was likewise efficient, resulting in a 43% inhibition in the stimulated proliferation of HB8521 cells as well as a 38% inhibition in the expression of a major functional cytokine interleukin-2 (IL-2), indicating the effective T cell anergy induced by gene therapy.

1. Introduction

Lymphocytes play a crucial role in regulating immune responses to infectious diseases, cancer, organ transplantation and autoimmune diseases [1,2]. Since most circulating lymphocytes in the peripheral blood are T cells that carry out a substantial part of immune responses [1], immunomodulation of T cells directly affects many pathological processes and provides tremendous potential in clinical treatment. It is well known that the traditional immunosuppressive agents such as Cyclosporine A (CsA) can induce immunosuppression and anergy in T cells. These agents work well in graft rejection and autoimmune diseases. However, they are usually associated with narrow therapeutic index and considerable toxicity [3,4]. Moreover, traditional immunosuppressive agents cannot provide sustained efficacy and therefore require life-long medication that may result in patient susceptibility to tumorigenesis, infections and other side effects [4,5]. In contrast, gene therapy can provide a better option to achieve immunosuppression of T cells with durability, less toxicity and cost-effectiveness [6]. Unfortunately, recent investigations have revealed that T cells are refractory to most of the current viral and nonviral gene delivery techniques, and the resistance of T cells to gene transfer has been a great challenge both *in vitro* and *in vivo* [1,2,7–10]. So far, viral vectors are mostly used to deliver genes into lymphocytes but their efficiency is generally low while safety risks such as immunogenicity are relatively high [2]. Nanomedicines such as polymeric systems complexed with nucleic acids have been developed and considered as one of the next generation therapeutics for immunotherapy [11].

Diacylglycerol (DAG) is a small organic molecule that positively regulates Ras-GRP and protein kinase Cθ activities, which is critical during T cell development and DAG-dependent signaling pathways after T cell receptor (TCR) stimulation. Since the diacylglycerol kinases (DGKs) are responsible for the phosphorylation of DAG into phosphatidic acid, overexpression of DGK could impair TCR signaling and consequently result in the anergy of T cells [12,13]. Therefore, the objective of the present research is to develop a nonviral agent that may efficiently deliver DGK gene into T cells in order to suppress their immune response function.

* Corresponding author. Fax: +86 20 85252276.
** Corresponding author. Fax: +86 20 84112245.
E-mail addresses: chgh1955@263.net (G. Chen), shuaixt@mail.sysu.edu.cn (X. Shuai).
[1] These authors contributed equally to this work.

0142-9612/$ – see front matter © 2009 Elsevier Ltd. All rights reserved.
doi:10.1016/j.biomaterials.2008.12.043

In mature T cells, engagement of the T cell antigen receptors such as CD3 receptor could lead to anergy induction and such receptors may also mediate potentially targeted gene delivery to T cells. Meanwhile, the clinically available MRI techniques possess great advantages in noninvasively monitoring therapeutic outcomes and targeting event both *in vitro* and *in vivo*, which recently has initiated the development of dual-purpose probes combining the gene or drug therapeutic and MR imaging functions. Among several reports available thus far in this topic, Gao et al. first reported the MRI-visible nanoparticulate systems for anti-cancer drug delivery *in vitro* [14] and Hyeon et al. described the quantum-dots-assisted optical imaging function for drug delivery [15]. As to the MRI-visible nucleic acid delivery in gene therapy, Moore et al. attached siRNA to magnetic nanoparticles and then used high-resolution MRI to carry out the simultaneous imaging of siRNA transfection *in vivo* [16]. Inspired by these latest progresses, we attempted the incorporation of the noninvasive MR imaging function into the T cell targeted gene delivery system. We investigated the application of this dual-purpose (i.e. therapy and imaging) probe for transfecting a rat T lymphocyte line with the DGK gene as well as the potential of using MRI to determine the targeted gene delivery *in vitro*.

2. Materials and methods

2.1. Materials

Synthesis of the nonviral delivery agents (PEG-*g*-PEI, PEG-*g*-PEI-SPION and $scAb_{CD3}$-PEG-*g*-PEI-SPION) was described in detail in Supplementary information. Cell culture media and fetal bovine serum (FBS) were purchased from Invitrogen Corporation (Carlsbad, CA, USA). Fluorescent staining agents 4′,6-diamidino-2-phenylindole (DAPI), popo-3, Oregen Green 488 were purchased from Molecular Probes, Inc. (Eugene, US). CD3 antibody was purchased from BD Bioscience Pharmingen (San Jose, CA, US). HB8521 cell, a rat T lymphocyte line, was ordered from American Type Culture Collection (ATCC, Manassas, VA). The plasmids pAAV-EGFP expressing green fluorescent protein and pcDNA3.1-DGK-flag were used in this study. Rat DGKα cDNA was amplified by RT-PCR using rDGKα F (5′-GATC-CACGATGACTGTCTGCAG-3′) and rDGKα R (5′-GAACACGGAGGCAGGATATGAT-3′) primer pairs. The PCR products were digested and cloned in-frame with a FLAG tag coding sequence at the N terminus into pcDNA3.1. The ultrapure plasmid DNAs (pDNAs) were prepared from *Escherichia coli* according to the manufacturer's instructions of EndoFree Plasmid Giga Kits (QIAGEN, CA, USA). To determine the yield, DNA concentration was determined by UV spectrophotometry at 260 nm. The purified pDNAs were kept in endotoxin-free TE buffer at a concentration of 2.4 μg/μL.

2.2. Polyplex formation

pDNA (4 μg) and an appropriate amount of delivery agent (PEG-*g*-PEI, PEG-*g*-PEI-SPION, or $scAb_{CD3}$-PEG-*g*-PEI-SPION) were dissolved separately in 0.9% sodium chloride solution. The two solutions were mixed by vigorous pipetting, and then the mixture was kept at room temperature for 60 min to allow polyplex formation. The amount of delivery agent used to complex pDNA was determined based on the designed experimental N/P ratios, which were calculated as the number of nitrogen atoms in delivery agents over that of the phosphate groups in pDNA. In the present work, polyplexes for the study on reporter gene transfection were prepared at N/P 10 (Fig. 1).

2.3. Determination of DNA complexation by gel retardation assay

In order to assess the pDNA condensation ability of the delivery agents, gel electrophoresis was performed on a Bio-Rad Sub-Cell electrophoresis cell (Bio-Rad Laboratories, Inc., US) and images were obtained on a DNR Bio-Imaging Systems (DNR Bio-Imaging Systems Ltd., Israel). Complex formation was induced at various N/P ratios from 1.7 to 2.5 in a final volume of 6× agarose gel loading dye mixture (i.e. 10 μL). pDNA and the appropriate amount of delivery agent were dissolved separately in a neutral solution containing 0.9% sodium chloride. The two solutions were mixed by vigorous pipetting, loaded onto the 0.9% agarose gels with ethidium bromide (0.1 μg/mL), and ran with Tris–acetate (TAE) buffer at 100 V for 40 min. DNA band shifts were revealed by irradiation with UV light.

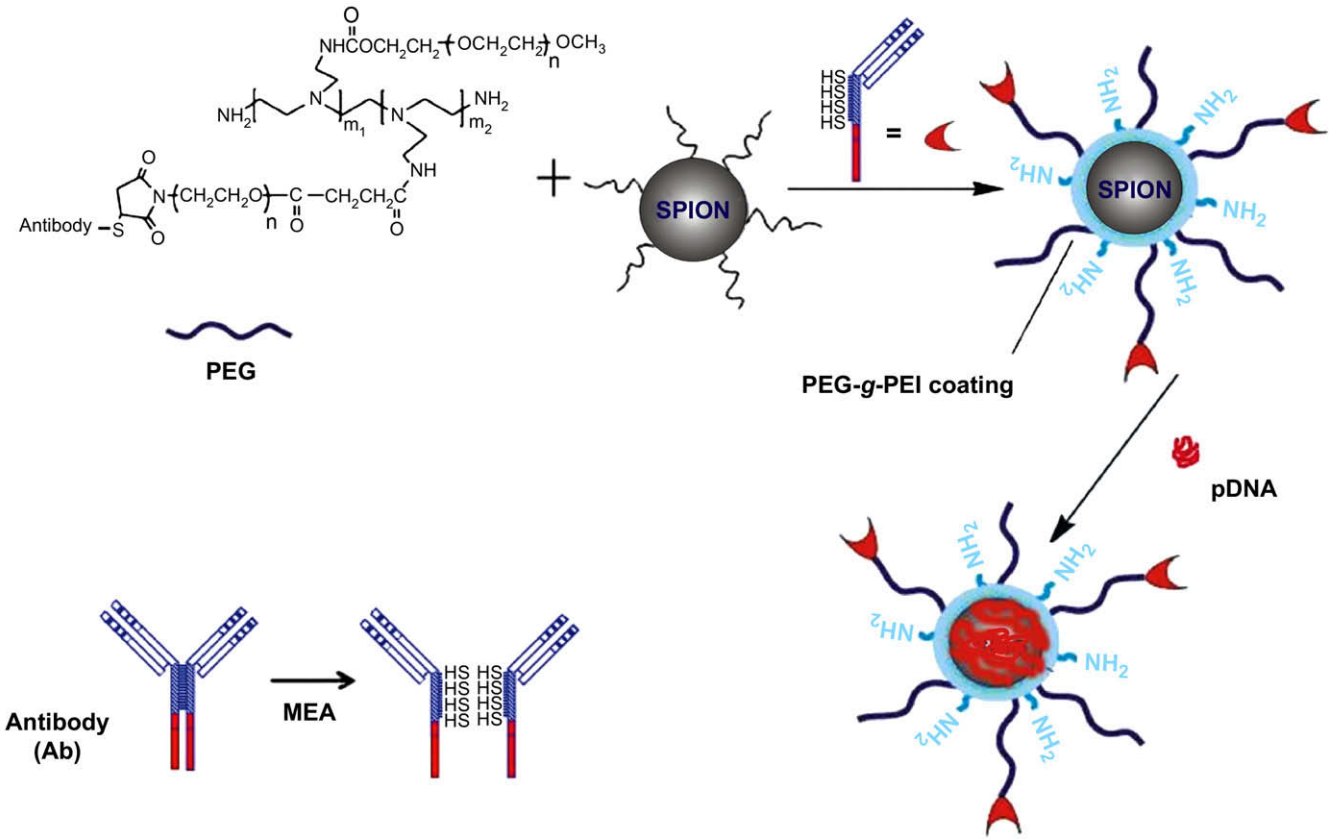

Fig. 1. Schematic formation process of magnetic targeting polyplex $scAb_{CD3}$-PEG-*g*-PEI-SPION/pDNA.

2.4. In vitro cytotoxicity assay

Cytotoxicity of the polyplexes with and without SPION encapsulation was evaluated using the WST-8 assay with Cell Counting Kit-8 (Dojindo, Kumamoto, Japan), as described in the manufacturer's manual. All experiments were conducted in triplicate and the following vectors were tested to assess the polyplex cytotoxicity: PEI, PEG-*g*-PEI, PEG-*g*-PEI-SPION, $scAb_{CD3}$-PEG-*g*-PEI and $scAb_{CD3}$-PEG-g-PEI-SPION. Polyplexes, i.e. the pDNA complexes, for cytotoxicity test were formed at various N/P values. HB8521 cells were seeded in 96-well plates at a density of 1×10^6 cells/well. RPMI-1640 cell culture medium (0.2 mL) was added to each well, and the pDNA mass in each well was set to 0.15 μg. After cell incubation for 48 h in the presence of polyplex, 10 μL of WST-8 solution was added. The cells were further incubated for 8 h, and the absorbance at 570 nm and 690 nm was recorded on a Tecan Infinite F200 Multimode plate reader.

2.5. Fluorescence labeling of PEI and pDNA and study on cellular uptake of polyplexes

Multiple fluorescence labeling of polyplexes for confocal laser scanning microscopy (CLSM) experiments was first completed. Oregon Green 488, an amine-reactive dye, was dissolved in dimethyl sulfoxide at 1 mg/mL. The delivery agent such as $scAb_{CD3}$-PEG-*g*-PEI-SPION was dissolved in 1 mL of 0.1 M sodium bicarbonate buffer (pH 8.3–9.0). Under agitation, the solution of reactive dye was slowly added into the solution of delivery agent. The mixture was maintained in dark and stirred for 1 h at room temperature. The unreacted labeling reagent was eliminated from the solution by ultrafiltration in an Amicon cell (regenerated cellulose membrane, MWCO = 5 kDa). By this way, the dye-delivery agent conjugate was washed several times with PBS of pH 7.4 until no absorption at 488 nm was detectable in the filtrate. pDNA was labeled in PBS of pH 7.4 with popo-3 (1 mg/mL in dimethyl sulfoxide, Molecular Probes) according to the manufacturer's manual. After the popo-3 solution was added into the pDNA solution, the mixture was stirred in dark for 1 h at room temperature. The pDNA–popo-3 conjugate was purified by gel filtration using Sephadex G-25 (Illustra MicroSpin G-25 Columns) with a commercial kit (GE Healthcare UK Limited, Buckinghamshire, UK).

HB8521 cells were seeded at a density of 1×10^6 cells per well in 6-well plates. The Cy3 labeled pDNA (4 μg) was complexed with the appropriate amount of Oregon Green-labeled delivery agent (e.g. 10 μg) as already described. The polyplex thus prepared was added into the RPMI-1640 cell culture medium. After 0.5 h, cells were washed 3 times with fresh PBS free of polyplex, fixed by incubation in the presence of 4% paraformaldehyde solution for 20 min, washed again for 3 times with fresh PBS, and further incubated for another 20 min after adding the DNA-staining agent DAPI dissolved in ultrapure water (1 mg/mL). Cells were isolated by centrifugation followed by discarding the supernatant, and then fresh PBS was added to resuspend the cells. The cell suspension was pipetted onto the glass slide and allowed to dry in ambient conditions. For excitation of DAPI fluorescence, an Enterprise UV laser with an excitation wavelength 358 nm was used. Excitation of Oregon Green was performed using an argon laser with an excitation wavelength of 488 nm, and for excitation of popo-3 a helium–neon laser with an excitation wavelength of 534 nm was used. CLSM observations were carried out using a Zeiss LSM 510 META microscope (Carl Zeiss Co., Ltd., Gottingen, Germany).

For the free ligand competitive inhibition assay, cells were pre-treated with large amount of free CD3 antibody (10× molar amount of $scAb_{CD3}$) for 30 min before the targeting micelles were added to the culture medium [17].

2.6. In vitro MRI scan

HB8521 cells, seeded at a number of 1×10^6 cells per well in 6-well plates, were incubated for 1 h in the presence of polyplex-containing SPION at Fe concentrations of 5, 10, 20, 40, 80 μg/mL in RPMI-1640 media, washed with PBS and then scanned with a 1.5 T MR scanner (GE Healthcare UK Limited, Buckinghamshire, UK) at room temperature. A circular surface coil with an inner diameter of 11 cm was used for all studies. T_2-weighted images were acquired using the following parameters: TR/TE, 5000/100 ms; FOV, 150 mm; matrix, 256 × 256; slice thickness, 1.5 mm. The MRI signal to noise ratios were measured. The increase of relaxation rate (s^{-1}, $1/T_2$) with increasing Fe concentration was analyzed by linear regression analysis. T_2 relaxivity, r_2 (s^{-1} mM^{-1}) was calculated as the slope of relaxation rate *vs* Fe concentration relationship.

2.7. Transfection experiments

Transfection experiments were performed in 6-well plates with 4 μg of either pAAV-EGFP or pcDNA3.1-DGK-flag per well. HB8521 cells were seeded at a density of 1×10^6 cells per well in RPMI-1640 medium. Polyplexes such as $scAb_{CD3}$-PEG-*g*-PEI-SPION/DNA, PEG-*g*-PEI-SPION/DNA, $scAb_{CD3}$-PEG-*g*-PEI/DNA, and PEG-*g*-PEI/DNA formed at designed N/P ratios were added into the media. After 8 h, the medium was replaced with fresh RPMI-1640 medium, and cells were further incubated for 40 h before measuring gene transfection level. For the reporter gene expression at N/P 10, cells were observed on a Carl Zeiss Aviox-1 inverted fluorescence microscope and then quantitatively analyzed using a FACScan flow cytometer. Western blotting with anti-DGKα antibody (Santa Cruz Biotechnology Inc., USA) was conducted to evaluate the expression level of therapeutic gene at N/P 3, 5, 10. Reporter gene transfection mediated by the magnetic delivery vectors conjugating half amount of CD3 single chain antibody, i.e. 1/2$scAb_{CD3}$-PEG-*g*-PEI-SPION/pAAV-EGFP and 1/2$scAb_{CD3}$-PEG-*g*-PEI/pAAV-EGFP, was performed as well.

Free ligand competitive inhibition in reporter gene transfection was evaluated. In this experiment, cells were pre-treated with a large amount of free CD3 antibody for 30 min before $scAb_{CD3}$-PEG-*g*-PEI-SPION/pAAV-EGFP or $scAb_{CD3}$-PEG-*g*-PEI/pAAV-EGFP was added into the medium. Cells were incubated for 8 h in the polyplex-containing medium and then for 40 h in the polyplex-free medium, as already described. The level of reporter gene expression was quantified by flow cytometry.

2.8. In vitro T cell anergy

The HB8521 cells were seeded in 96-well plates at a density of 5×10^5 cells per well in RPMI-1640 medium. After transfection with polyplex for 48 h, cells were stimulated with PMA (50 ng/mL) plus ionomycin (200 ng/mL) and then incubated for another 40 h at 37 °C in 5% CO_2 atmosphere, during which the culture media in the wells were collected for measuring the expression of the functional cytokine IL-2 by a solid phase sandwich enzyme linked immunosorbent assay (ELISA) using Biosource immunoassay rat IL-2 kit according to the manufacturer's instruction (Invitrogen, USA). [^{3}H]thymidine was added to the culture media at a concentration of 1 μCi/well, and then the cells were incubated for 8 h. Subsequently, the cell proliferation was determined according to literature reports [6,18]. The cells were collected onto filters with a cell harvester. ^{3}H incorporation was measured on a Beckman Liquid Scintillation Counter (Beckman Coulter, Inc., USA). All assays were performed in quadruplicate.

2.9. Statistical analysis

Statistical analysis of Data was performed with the one-factor analysis of variance (SPSS software, version 13.0, SPSS Inc). The results were expressed as mean ± SE, and $P < 0.05$ was considered to be statistically significant. All statistical tests were two-sided.

3. Results

3.1. Synthesis of PEG-g-PEI-SPION and formation of polyplex

Synthesis of PEG-*g*-PEI and PEG-*g*-PEI-SPION was described in detail in Supplementary information. PEG-*g*-PEI was synthesized by conjugating CDI-activated PEG to PEI. PEG-*g*-PEI-SPION was successfully synthesized by "ligand exchange" method [19]. In this approach, the cationic copolymer PEG-*g*-PEI replaced the hydrophobic coating of oleic acid/oleylamine on the surface of SPION nanoparticles measuring 6 nm. The SPION weight percentage in the polymer-coated nanoparticles was determined to be 55% by Fe atomic absorption assay (Supplementary information). The dispersion of the obtained complex PEG-*g*-PEI-SPION in water is stable.

Agarose gel electrophoresis was conducted to confirm the pDNA complexation ability of PEG-*g*-PEI and PEG-*g*-PEI-SPION. It is well known that the complexation of pDNA with cationic polymers is due to the electrostatic neutralization, by which DNA partially or completely loses the negative charge and consequently loses the mobility in the electric field. Therefore, the retardation of DNA mobility in gel electrophoresis can be checked as a measure of the polymer ability to complex DNA. As shown in Fig. 2, both PEG-*g*-PEI and PEG-*g*-PEI-SPION started to form complexes from low N/P ratios (e.g. 1.7). Compared to the naked DNA control, less DNA migrated into the gel upon complexation with delivery agents. DNA condensation by both PEG-*g*-PEI and PEG-*g*-PEI-SPION completely retarded the DNA motion at almost the same N/P ratio around 2.3, indicating the complexation of full DNA chains [20]. These results demonstrated that the effect of pre-complexation of SPION on the DNA complexation capacity of PEG-*g*-PEI was almost neglectable. This notion is reasonable considering the high positive charge of PEG-*g*-PEI-SPION particles.

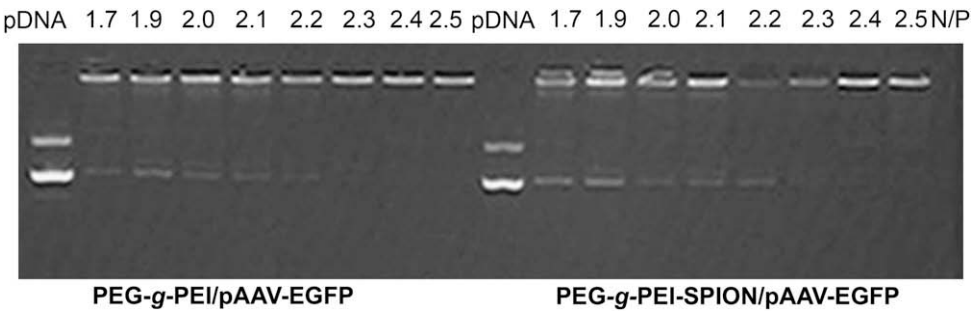

Fig. 2. Determination of pDNA condensation by gel retardation assay. Plasmid DNA is complexed with PEG-*g*-PEI-SPION (right) or PEG-*g*-PEI (left) at various N/P ratios and loaded into an agarose gel. Complexation prevents DNA migration into gel.

3.2. *In vitro* cytotoxicity

As demonstrated in the gel electrophoresis test (Fig. 2), the N/P value significantly affected the DNA condensation efficiency. However, higher N/P values not only led to better DNA condensation but also resulted in higher positive charge of the polyplex nanoparticle surface (Supplementary information, Table S1). Although a positive charge is well known to facilitate the cell uptake of nanoparticles through a nonspecific electrostatic interaction between the nanoparticles and negatively charged cell membranes, it is also a major underlying cause for cytotoxicity. Gene delivery mediated by nonviral vectors usually applies polyplexes with higher N/P ratios providing that the cytotoxicity is still acceptable at these N/P ratios. Therefore it is important to check on the cytotoxicity of polyplexes formed at different N/P values. In the present research, WST-8 assay was employed to determine the cytotoxicity of polyplexes. To make the data comparable, the applied DNA amount per well in cell culture was set constantly to 0.15 μg. As shown in Fig. 3, polyplexes based on all the PEG-modified polyplexes displayed much lower cytotoxicity in HB8521 cells than the control based on PEI 25 kDa at any of the N/P values from 5 to 30. This information is meaningful because the gel electrophoresis experiment has demonstrated that full DNA complexation can be achieved at N/P 2.3. Therefore, at the N/P range from 5 to 30, a full pDNA condensation while a reduced cytotoxicity in PEG-modified polyplexes compared to the neat PEI-based control can be expected. Neither $scAb_{CD3}$ nor SPION existing in the polyplex obviously influences the cytotoxicity. With the N/P increase from 5 to 10, the PEI-based control group induced significant decrease in cell viability, whereas comparable decrease in cell viability was not observed with polyplexes based on the four PEG-modified delivery agents. As N/P ratio reached 10, cells retained about 75% viability when transfected with polyplexes based on PEG-modified delivery agents, while about 70% cells were killed when transfected with the polyplex based on PEI 25 kDa. At an even higher N/P ratio of 20, the cell viability for all groups was significantly lower. Based on these results, the current research uses polyplexes formed at N/P 10 for the studies on cellular uptake and gene transfection.

3.3. *Internalization of polyplexes into HB8521 cells*

We conducted multiple fluorescent labeling of pDNA and delivery agent, and then investigated the uptake of polyplexes by HB8521 cells after 1 h incubation using confocal laser scanning microscopy (CLSM). For a better visualization of the intracellular distribution of polyplexes, the nuclei were stained blue with the DNA-staining agent DAPI. Cell uptake efficiency of polyplexes without targeting ligand modification, PEG-*g*-PEI-SPION/DNA and PEG-*g*-PEI/DNA, was very low as only strong blue fluorescence from the nuclei was observed (Fig. 4c and f). In comparison, the targeting polyplexes, both $scAb_{CD3}$-PEG-*g*-PEI-SPION/DNA and $scAb_{CD3}$-PEG-*g*-PEI/DNA, were efficiently taken up by the cells leading to very strong and overlapped green and red fluorescence (Fig. 4a and d). Moreover, a pre-incubation of cells with an excessive amount of free CD3 antibody significantly inhibited the internalization of the two targeting polyplexes into the cells. Cells thus pre-treated only displayed strong blue fluorescence of nuclei (Fig. 4b and e). These results demonstrated that endocytosis of $scAb_{CD3}$-PEG-*g*-PEI-SPION/DNA and $scAb_{CD3}$-PEG-*g*-PEI/DNA polyplexes was mediated by the specific interaction between the $scAb_{CD3}$ and CD3 receptors, and consequently modification of polyplexes with $scAb_{CD3}$ can significantly enhance their cellular uptake by T cells.

As shown in Fig. 5, the MRI signal intensity to noise ratio (SNR) of HB8521 cells incubated with polyplexes decreased in varied degrees in T_2-weighted MR imaging depending on the Fe concentration in cell culture as well as the presence/absence of targeting ligand in polyplexes. Such decrease in signal intensity became more significant when the iron concentration in culture media was higher. While the MRI signal intensity of cells incubated with the nontargeting polyplex (PEG-*g*-PEI-SPION/pDNA) in T_2-weighted imaging decreased as well at various Fe concentrations, the MRI signal intensity of cells incubated with the targeting one ($scAb_{CD3}$-PEG-*g*-PEI-SPION/pDNA) exhibited much more significant decrease at every Fe concentration above 10 μg/mL. As one of the most important molecular imaging technologies at present, MRI possesses the advantage of excellent sensitivity and spatial

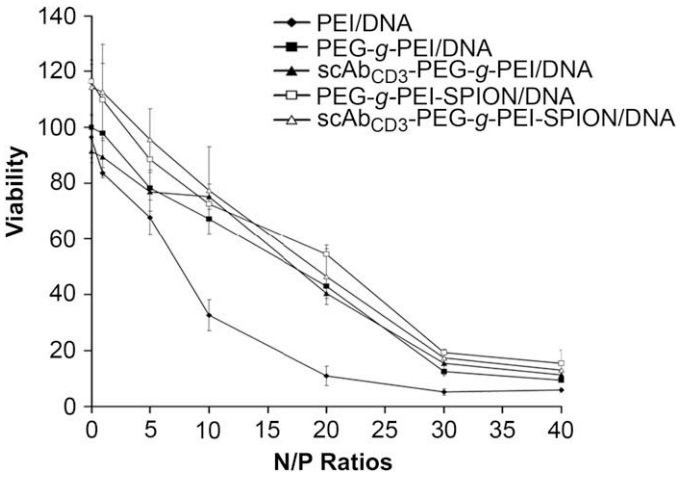

Fig. 3. *In vitro* cytotoxicity of polyplexes in HB8521 cells determined with WST-8 assay. For cell culture, pDNA concentration was set constantly to 0.15 μg per well (0.2 mL medium) and the polyplex amount applied to each well was determined accordingly based on N/P ratios. Results are means ± SD ($n = 3$).

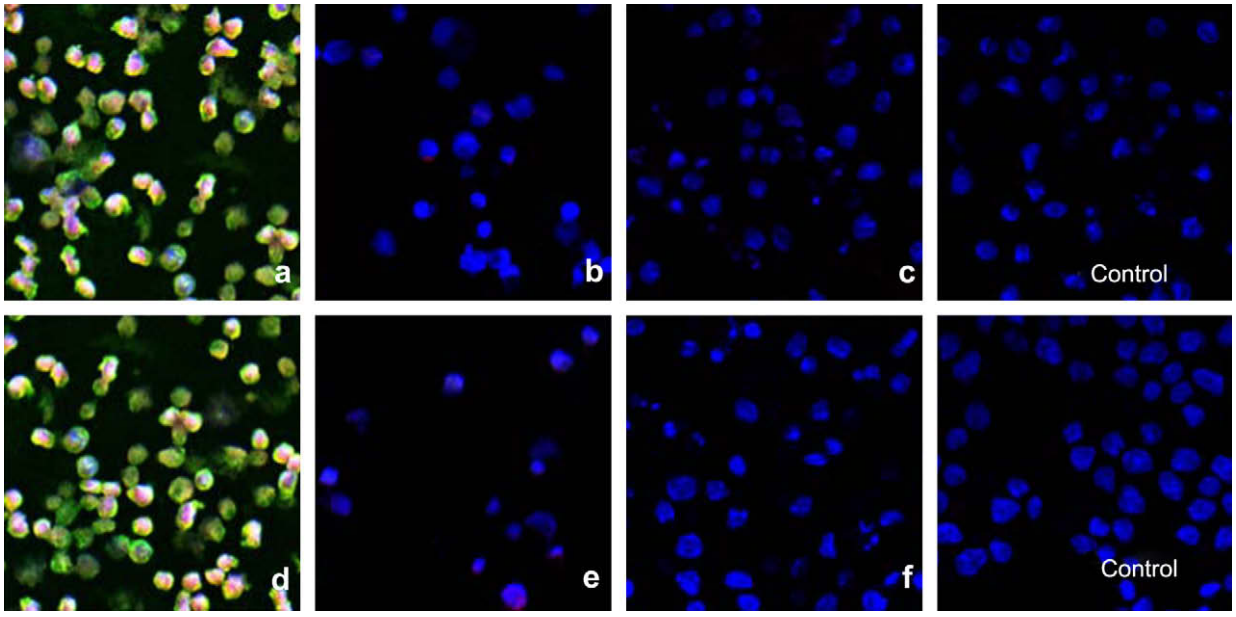

Fig. 4. Laser confocal microscopic images (100×) of HB8521 cells after 1 h incubation with scAb$_{CD3}$-PEG-*g*-PEI-SPION/pAAV-EGFP (a), scAb$_{CD3}$-PEG-*g*-PEI/pAAV-EGFP (d), PEG-*g*-PEI-SPION/pAAV-EGFP (c) and PEG-*g*-PEI/pAAV-EGFP (f); HB8521 cells after 30 min incubation with free CD3 antibody, and then incubated with scAb$_{CD3}$-PEG-*g*-PEI-SPION/pAAV-EGFP (b) or scAb$_{CD3}$-PEG-*g*-PEI/pAAV-EGFP (e) for 30 min in RPMI-1640 medium in comparison with normal HB8521 cells (control). All polyplexes were formed at N/P 10.

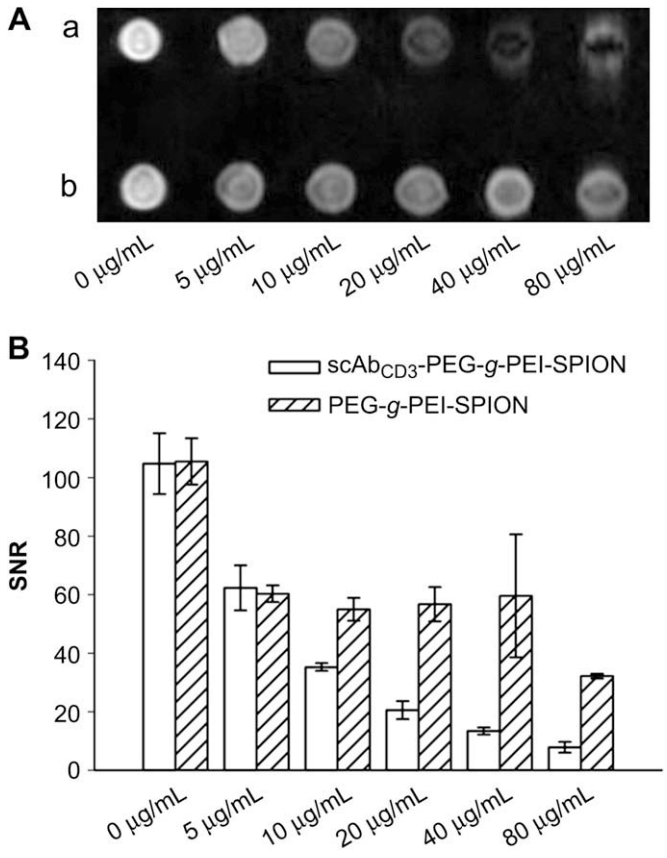

Fig. 5. Fast relaxation fast spin echo sequence (FRFSE) T_2-weighted imaging of HB8521 cells after 1 h incubation with scAb$_{CD3}$-PEG-*g*-PEI-SPION/pAAV-EGFP (a) and PEG-*g*-PEI-SPION/pAAV-EGFP (b) respectively at Fe concentrations of 0, 5, 10, 20, 40, 80 μg/mL in RPMI-1640 medium; Cells were scanned with a 1.5 T MRI scanner at room temperature. Polyplexes were formed at N/P 10. B shows the MRI signal intensity to noise ratios at various Fe concentrations ($n = 3$).

resolution allowing imaging even in cell level. Furthermore, it can be used as a noninvasive strategy to monitor the targeted delivery efficiency of drugs or nucleic acids given that the delivery vectors were constructed MRI-visible. In light of such knowledge, we embedded SPION into the gene delivery agents in the present research. It was noted that, during the course of the present research, the delivery of reporter gene into cancer cells *in vitro* using SPION-conjugated PEI as a delivery agent was reported by Pun et al. [21]. They demonstrated that the DNA packaging with SPION-complexed PEI resulted in enhanced MRI sensitivity. Increase in MRI sensitivity was also obtained with SPION-complexed PEG-*g*-PEI upon DNA complexation (Supplementary information, Fig. S4).

3.4. Gene transfection efficiency

After the HB8521 cells were incubated in the presence of polyplexes containing either reporter gene plasmid (pAAV-EGFP) or therapeutic gene plasmid (pcDNA3.1-DGKα), transgene expression level was assessed. Expression of reporter gene in T cells after transfection was observed with inverted fluorescence microscope and quantified by flow cytometry (Fig. 6). Targeting polyplexes showed much stronger green fluorescence than their nontargeting counterparts no matter whether SPION was encapsulated or not, as shown in Fig. 6 (b *vs* f and d *vs* h). The observation, shown in Fig. 6 (b *vs* d), that SPION did not obviously affect the transgene expression of polyplexes in HB8521 cells is consistent with the results discussed in previous sections, i.e. SPION did not obviously affect pDNA complexation of delivery agents and the cell uptake of polyplexes. Reporter gene transfection in HB8521 cells with nontargeting polyplexes was at very low levels. As shown in Fig. 6a, quantitative flow cytometric analysis indicated that the transfection efficiency in HB8521 cells with PEG-*g*-PEI/pDNA and PEG-*g*-PEI-SPION/pDNA was only $5.60 \pm 1.45\%$ and $7.39 \pm 2.21\%$ respectively ($P < 0.05$). In comparison, the gene transfection efficiency was remarkably increased to $75.78 \pm 5.5\%$ and $81.95 \pm 5.73\%$ respectively upon scAb$_{CD3}$-functionalization of PEG-*g*-PEI/pDNA and PEG-*g*-PEI-SPION/pDNA ($P < 0.05$). Moreover, the transgene

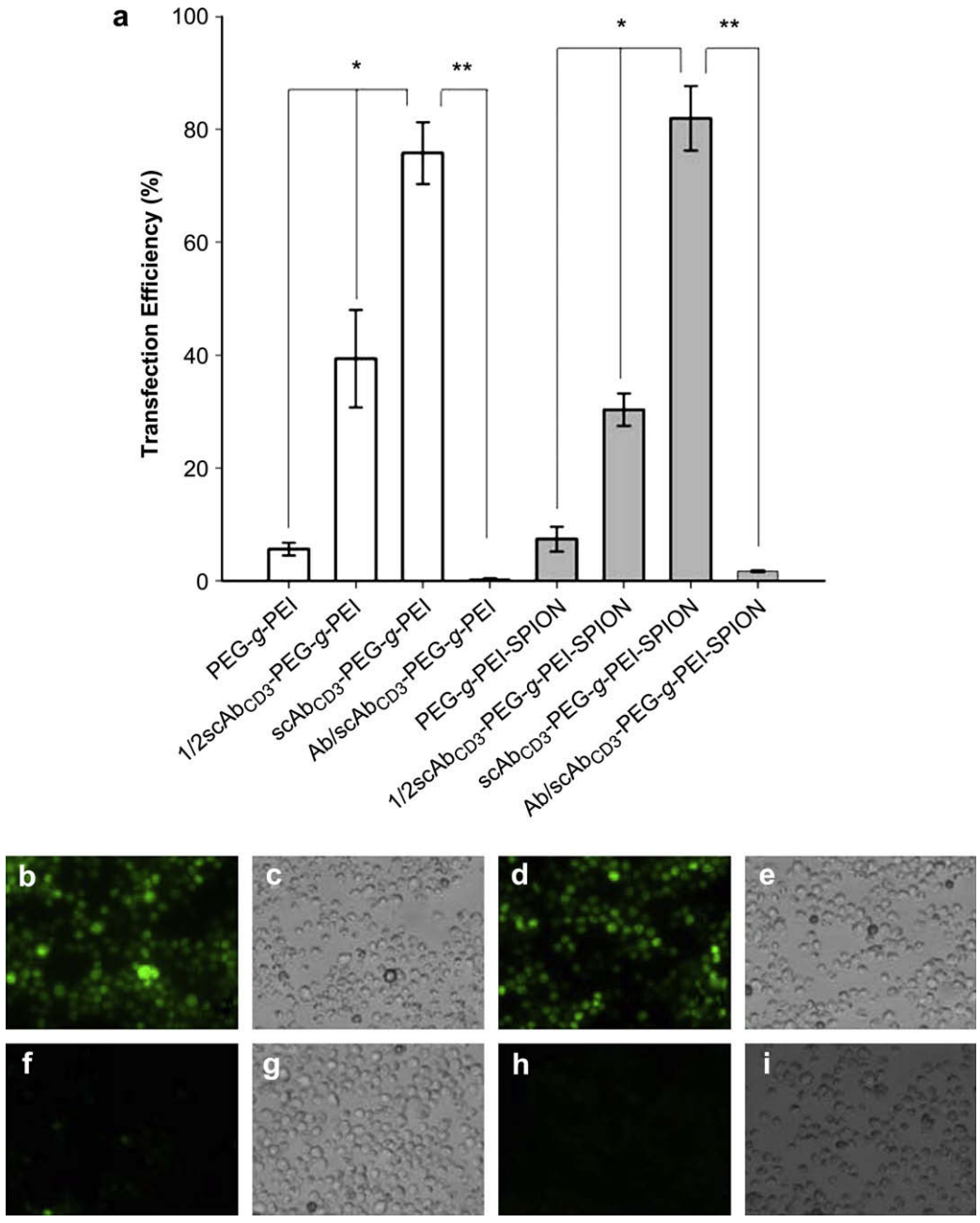

Fig. 6. (a) Relative transfection efficiency of reporter gene in HB8521 cells determined by flow cytometry ($n = 3$). The fluorescent and bright field microscopic images of cells incubated with $scAb_{CD3}$-PEG-*g*-PEI-SPION/pAAV-EGFP (b and c), PEG-*g*-PEI-SPION/pAAV-EGFP (f and g), $scAb_{CD3}$-PEG-g-PEI/pAAV-EGFP (d and e), and PEG-*g*-PEI/pAAV-EGFP (h and i). Polyplexes were formed at N/P 10. $^{*}P < 0.05$; $^{**}P < 0.01$.

expression in transfected cells depended on the $scAb_{CD3}$ density in polyplexes. When the $scAb_{CD3}$ density in polyplexes was decreased by half, gene transfection efficiency of $scAb_{CD3}$-PEG-*g*-PEI-SPION/pDNA and $scAb_{CD3}$-PEG-*g*-PEI/pDNA was decreased to $30.33 \pm 2.86\%$ and $39.35 \pm 8.65\%$ respectively.

The expression of the therapeutic DGKα gene was examined by western blotting. DGKα protein concentration in transfected HB8521 cells was analyzed by immunoblotting with an antibody specific for DGKα protein. Obvious protein straps were observed indicating the expression of DGKα protein in HB8521 cells after transfection with various polyplexes as shown in Fig. 7. For each polyplex, three different N/P values 3, 5 and 10 were tested. Targeting polyplexes at all three N/P values showed much more significant enhancement in DGKα protein expression in HB8521 cells in comparison with their nontargeting counterparts. Interestingly, SPION existence in polyplexes seemed to improve expression of DGKα as well for both the targeting and nontargeting pairs, i.e. $scAb_{CD3}$-PEG-*g*-PEI-SPION/pDGKα *vs* $scAb_{CD3}$-PEG-*g*-PEI/pDGKα and PEG-*g*-PEI-SPION/pDGKα *vs* PEG-*g*-PEI/pDGKα. In addition, the level of DGKα expression depended much on the N/P value of polyplex. Among the three N/P ratios employed in transfection, the DGKα/β-actin optical density ratio in transfected cells reached the highest at N/P 10 for most of the studied polyplexes, which represented once again the rationale of using polyplexes formed at N/P 10 to transfect T lymphocytes and induce anergy as will be reported in the next section.

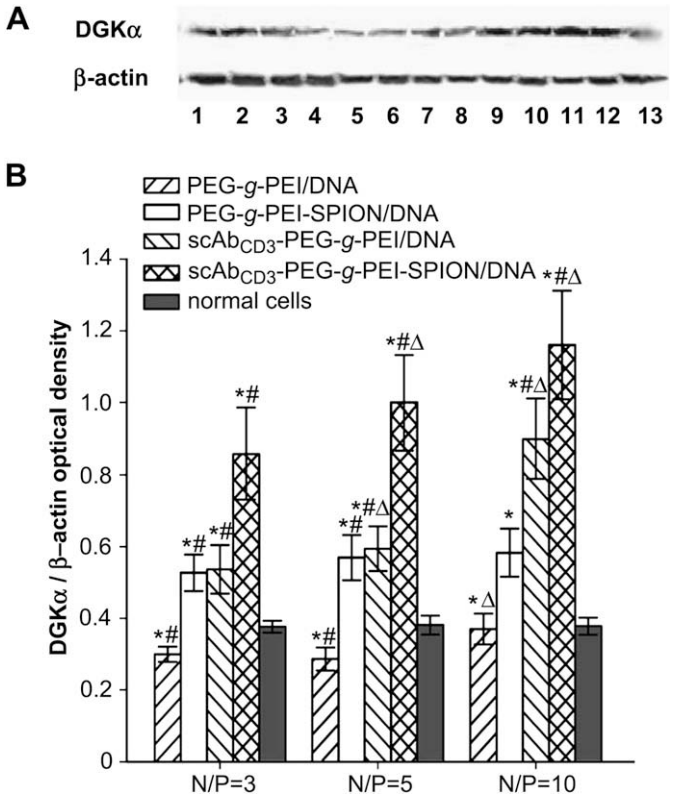

Fig. 7. DGKα expression levels in HB8521 cells determined by immunoblotting (A). Lanes 1–3: PEG-*g*-PEI-SPION/pDNA; lanes 4–6: PEG-*g*-PEI/pDNA; lanes 7–9: $scAb_{CD3}$-PEG-*g*-PEI/pDNA; lanes 10–12: $scAb_{CD3}$-PEG-*g*-PEI-SPION/pDNA; lane 13: normal cells. For each polyplex group, three N/P ratios were tested (3, 5, 10 from left to right). The DGKα/β-actin optical density ratios ($n = 3$) were shown in B. $^{*}P < 0.05$ (targeting *vs* nontargeting, same N/P and SPION encapsulation); $\#P < 0.05$ (with SPIO *vs* without SPIO, same N/P and ligand targeting); $\Delta P < 0.05$ (compared with the same polyplex formed at N/P 3).

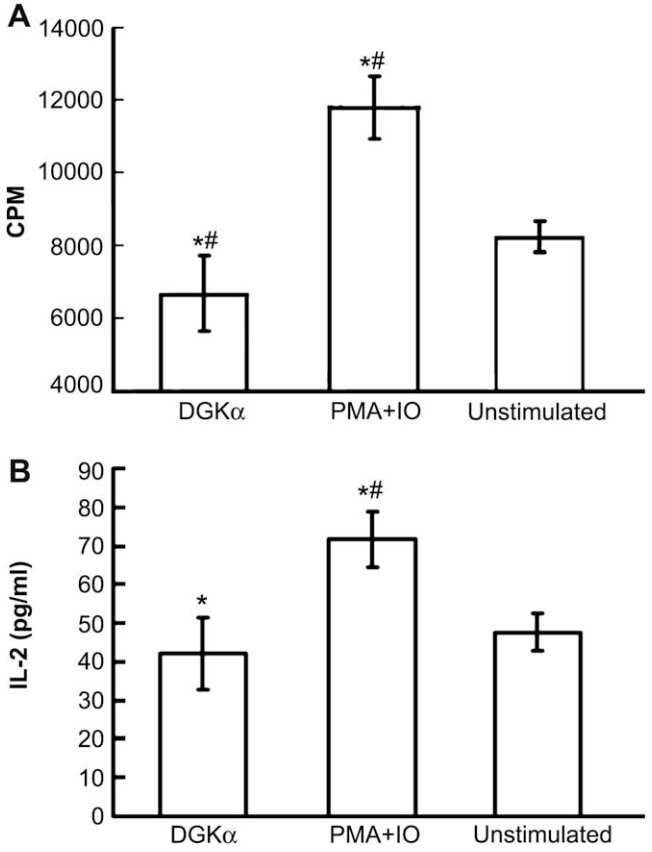

Fig. 8. HB8521 cell proliferation and anergy ($n = 3$) determined by [^{3}H]thymidine assay (A) and ELISA assay (B) respectively. Cells transfected with $scAb_{CD3}$-PEG-*g*-PEI-SPION/pcDNA3.1-DGKα showed less proliferation and IL-2 expression in response to stimulation of ionomycin and PMA than cells without pre-transfection while being stimulated. Polyplex formed at N/P 10 was used. $^{*}P < 0.05$, compared between DGKα and (PMA + IO) groups; $\#P < 0.05$, DGKα and (PMA + IO) groups *vs* unstimulated control.

3.5. *In vitro* T cell anergy assay

After DGKα gene was efficiently transferred into HB8521 cells, we tested whether increasing expression of DGKα in HB8521 cells would damp the TCR-induced DAG signaling [1] and consequently blunt the T cell proliferation and activation *in vitro*. As shown in Fig. 8A, HB8521 cells transfected with the magnetic targeting polyplex demonstrated much less proliferation in response to stimulation with ionomycin and PMA than cells without pre-transfection while being stimulated. Although stimulated, cells pre-transfected even showed less proliferation than normal cells without ionomycin and PMA stimulation. As expected, T cell anergy date revealed by ELISA accords with the cell proliferation results measured by the [^{3}H]thymidine assay. Upon ionomycin and PMA stimulation, HB8521 cells transfected with the magnetic targeting polyplex produced much less amount of IL-2, which is a major functional cytokine of T cells in response to stimulation such as organ transplantation [22], than the cells without pre-transfection with polyplex as shown in Fig. 8B. These results suggested that delivery of the therapeutic DGKα gene into T cells with our targeting delivery agents would effectively impair cell proliferation and induce T cell anergy *in vitro*. These data have encouraged us to begin the efficacy test in a liver transplant animal model.

4. Discussion

Gene delivery has been frequently used to analyze construction and function of mammalian cells, especially lymphocytes. Reported approaches for gene transfer include the electroporation, lipofection, calcium phosphate precipitation, nucleofection and viral gene delivery [1,2,7,8,9]. Although many inspiring results have been reported up to now, these approaches still have drawbacks in cost-effectiveness, efficiency and bio-safety. Recently, gene transfer with nonviral nanoparticles became a quickly developing strategy which can be used to modulate gene expression in targeted cells. One of the greatest advantages those nanoparticles possess over the viral vectors is the cell-type specificity after the chemical conjugation of a targeting ligand.

Among the variety of materials which have been utilized in the fabrication of nanoparticles for gene transfection, a cationic polymer polyethylenimine (PEI) can condense pDNA into compact nanoparticle possessing a unique endosomolytic activity for effective DNA release inside cells, i.e. the so called proton sponge effect, which makes PEI one of the most promising nonviral vectors. However, PEI-based gene transfection technology faced obstacle in cytotoxic effect which is usually correlated with molecular weight and concentration of the polymer, due to the electrostatic interactions of PEI with the negatively charged components of cell membranes such as sialic acid. Indeed, the strategies for gene therapy with nonviral vectors require not only high specificity but also minimal side effects. To this end, PEI has been modified with neutral hydrophilic polymers, in particular with poly(ethylene glycol) (PEG), to reduce cytotoxicity while maintaining considerable gene transfer efficiency [23–28]. PEG can shield the cationic

surface charge of PEI and in addition can suppress the nonspecific interactions of PEI with blood components (e.g. plasma proteins) and extracellular matrix [29,30]. Moreover, PEG-modified PEI can form nanoparticulate complex with superparamagnetic iron oxide Fe_3O_4 (SPION) which was known as a highly efficient T_2 contrast agent for magnetic resonance imaging (MRI), rendering the vector MRI-visible. Various targeting ligands such as antibodies can be easily introduced into the delivery vector through PEG linkage for active targeting tropism *in vivo*. By these means, the specific delivery of gene to the targeted cells was achievable and meanwhile the process of specific interaction with targeted cells and tissues could be tracked with the noninvasive MRI technique [31–33].

Here, we tried to modulate transgene expression in a rat T lymphocyte line, HB8521, using a type of MRI-visible targeting nanoparticles based on the PEG-grafted PEI copolymer (PEG-*g*-PEI) into which the MRI T_2 agent SPION and targeting ligand the CD3 single chain antibody were incorporated. Although gene transfection in T cells is generally a big challenge, we have significantly enhanced transgene expression in HB8521 cells *via* the CD3 receptor-mediated endocytosis of polyplexes. The same technique has been applied to primary T cells in our lab and initial results are promising as well (data not shown).

As SPION is a well-known excellent T_2 contrast agent for MRI, complexation of SPION in gene delivery agents potentially allows noninvasively monitoring of the delivery events both *in vivo* and *in vitro* with MRI scan [2,34], which has driven us to introduce SPION into gene delivery agents in the present work. Our ultimate goal is to develop a type of MRI-visible gene delivery vector whose active targeting efficiency can be noninvasively tracked *in vivo*. As the first step in our scheme, we have initially proved that the $scAb_{CD3}$-functionalized polyplex has better targeting tropism to T lymphocytes *in vitro* than its nontargeting counterpart, and the clinical 1.5 T MRI scanner has the potential to monitor this targeting event in a noninvasive way. We are currently conducting animal tests with the $scAb_{CD3}$-functionalized polyplexes to investigate their performance *in vivo*.

5. Conclusion

We established a new nonviral gene delivery agent bearing CD3 single chain antibody (scAbCD3) as a targeting ligand to T lymphocytes and MRI T_2 agent SPION. Molecular tailoring of these novel gene carriers to effectively transfer both the reporter and therapeutic genes to a rat T lymphocyte cell line was successfully demonstrated. Polyplexes based on these targeted delivery agents exhibited not only high efficacy of gene transfection in HB8521 cells but also low cytotoxicity. The strategy was successfully applied *in vitro* to inhibit proliferation and function of T lymphocytes. In comparison with other treatment regimens for transplant and autoimmune diseases, magnetic nanoparticles (MNPs) for targeting gene delivery may be a more useful approach in terms of preventing disease onset and/or disease progression. Our results revealed the great potential of this compound nano-system as a MRI-trackable and T-lymphocyte-targeted gene carrier in post-transplantation immunotherapy.

Acknowledgements

This work was supported by the Natural Science Foundation of China (Grant Nos. 20474076, 30571769, 20728403 and 50673103), the Natural Science Foundation of Guangdong Province (Grant No. 7003703), Postdoctoral Foundation of China (Grant No. 20070410250), and the Ph.D. Programs Foundation of Ministry of Education of China (Grant No. 20060558083).

Appendix

Figures with essential colour discrimination. Certain figures in this article, in particular parts of Figs. 4 and 6, are difficult to interpret in black and white. The full colour images can be found in the online version, at doi:10.1016/j.biomaterials.2008.12.043.

Appendix. Supplementary information

Supplementary data associated with this article can be found in the online version, at doi:10.1016/j.biomaterials.2008.12.043.

References

[1] Sharma S, Cantwell M, Kipps TJ, Friedmann T. Efficient infection of a human T-cell line and of human primary peripheral blood leukocytes with a pseudotyped retrovirus vector. Proc Natl Acad Sci U S A 1996;93:11842–7.
[2] Goffinet C, Keppler OT. Efficient nonviral gene delivery into primary lymphocytes from rats and mice. FASEB J 2006;20:500–2.
[3] Cattaneo D, Baldelli S, Perico N. Pharmacogenetics of immunosuppressants: progress, pitfalls and promises. Am J Transplant 2008;8:1374–83.
[4] Gunthart M, Kearns-Jonker M. Gene therapy for the induction of chimerism and transplant tolerance. Curr Gene Ther 2007;7:411–20.
[5] Horn PA, Figueiredo C, Kiem HP. Gene therapy in the transplantation of allogeneic organs and stem cells. Curr Gene Ther 2007;7:458–68.
[6] Gould DJ, Chernajovsky Y. Novel delivery methods to achieve immunomodulation. Curr Opin Pharmacol 2007;7:445–50.
[7] Volpers C, Kochanek S. Adenoviral vectors for gene transfer and therapy. J Gene Med 2004;6:S164–71.
[8] Kinyanjui MW, Ramos-Barbón D, Villeneuve A, Fixman ED. Enhanced transduction of antigen-stimulated T lymphocytes with recombinant retroviruses concentrated by centrifugal filtration. J Immunol Methods 2006;314:80–9.
[9] Tahvanainen J, Pykäläinen M, Kallonen T, Lähteenmäki H, Rasool O, Lahesmaa R. Enrichment of nucleofected primary human CD4 + T cells: a novel and efficient method for studying gene function and role in human primary T helper cell differentiation. J Immunol Methods 2006;310:30–9.
[10] Hozumi K, Ohtsuka R, Suzuki D, Ando K, Ito M, Nishimura T, et al. Establishment of efficient reaggregation culture system for gene transfection into immature T cells by retroviral vectors. Immunol Lett 2000;71:61–6.
[11] Jeong JH, Kim SW, Park TG. Molecular design of functional polymers for gene therapy. Prog Polym Sci 2007;32:1239–74.
[12] Olenchock BA, Guo R, Carpenter JH, Jordan M, Topham MK, Koretzky GA, et al. Disruption of diacylglycerol metabolism impairs the induction of T cell anergy. Nat Immunol 2006;7:1174–81.
[13] Zhong XP, Hainey EA, Olenchock BA, Zhao H, Topham MK, Koretzky GA. Regulation of T cell receptor-induced activation of the Ras-ERK pathway by diacylglycerol kinase zeta. J Biol Chem 2002;277:31089–98.
[14] Nasongkla N, Bey E, Ren J, Ai H, Khemtong C, Guthi JS, et al. Multifunctional polymeric micelles as cancer-targeted, MRI-ultrasensitive drug delivery systems. Nano Lett 2006;6:2427–30.
[15] Kim J, Lee JE, Lee SH, Yu JH, Lee JH, Park TG, et al. Designed fabrication of a multifunctional polymer nanomedical platform for simultaneous cancer-targeted imaging and magnetically guided drug delivery. Adv Mater 2008;20:478–83.
[16] Medarova Z, Pham W, Farrar C, Petkova V, Moore A. In vivo imaging of siRNA delivery and silencing in tumors. Nat Med 2007;13:372–7.
[17] Nasongkla N, Shuai X, Ai H, Weinberg BD, Pink J, Boothman DA, et al. cRGD-functionalized polymer micelles for targeted doxorubicin delivery. Angew Chem Int Ed Engl 2004;43:6323–7.
[18] Hermanson GT. Bioconjugate techniques. San Diego, Calif: Academic Press; 1996. p. 463–4.
[19] Tromsdorf UI, Bigall NC, Kaul MG, Bruns OT, Nikolic MS, Mollwitz B, et al. Size and surface effects on the MRI relaxivity of manganese ferrite nanoparticle contrast agents. Nano Lett 2007;7:2422–7.
[20] Wang DA, Narang AS, Kotb M, Gaber AO, Miller DD, Kim SW, et al. Novel branched poly(ethylenimine)–cholesterol water-soluble lipopolymers for gene delivery. Biomacromolecules 2002;3:1197–207.
[21] Park IK, Ng CP, Wang J, Chu B, Yuan C, Zhang S, et al. Determination of nanoparticle vehicle unpackaging by MR imaging of a T2 magnetic relaxation switch. Biomaterials 2008;29:724–32.
[22] Burchill MA, Yang J, Vang KB, Farrar MA. Interleukin-2 receptor signaling in regulatory T cell development and homeostasis. Immunol Lett 2007;114:1–8.
[23] Clamme JP, Krishnamoorthy G, Mély Y. Intracellular dynamics of the gene delivery vehicle polyethylenimine during transfection: investigation by two-photon fluorescence correlation spectroscopy. Biochim Biophys Acta 2003;1617:52–61.
[24] Fischer D, Bieber T, Li Y, Elsässer HP, Kissel T. A novel non-viral vector for DNA delivery based on low molecular weight, branched polyethylenimine: effect of molecular weight on transfection efficiency and cytotoxicity. Pharm Res 1999;16:1273–9.

[25] Fischer D, von Harpe A, Kunath K, Petersen H, Li Y, Kissel T. Copolymers of ethylene imine and *N*-(2-hydroxyethyl)-ethylene imine as tools to study effects of polymer structure on physicochemical and biological properties of DNA complexes. Bioconjug Chem 2002;13:1124–33.
[26] Fischer D, Osburg B, Petersen H, Kissel T, Bickel U. Effect of poly(ethylene imine) molecular weight and pegylation on organ distribution and pharmacokinetics of polyplexes with oligodeoxynucleotides in mice. Drug Metab Dispos 2004;32:983–92.
[27] Ogris M, Brunner S, Schüller S, Kircheis R, Wagner E. PEGylated DNA/transferrin–PEI complexes: reduced interaction with blood components, extended circulation in blood and potential for systemic gene delivery. Gene Ther 1999;6:595–605.
[28] Zalipsky S. Functionalized poly(ethylene glycol) for preparation of biologically relevant conjugates. Bioconjug Chem 1995;6:150–65.
[29] Lungwitz U, Breunig M, Blunk T, Göpferich A. Polyethylenimine-based non-viral gene delivery systems. Eur J Pharm Biopharm 2005;60:247–66.
[30] Ogris M, Walker G, Blessing T, Kircheis R, Wolschek M, Wagner E. Tumor-targeted gene therapy: strategies for the preparation of ligand–polyethylene glycol–polyethylenimine/DNA complexes. J Control Release 2003;91:173–81.
[31] Leakakos T, Ji C, Lawson G, Peterson C, Goodwin S. Intravesical administration of doxorubicin to swine bladder using magnetically targeted carriers. Cancer Chemother Pharmacol 2003;51:445–50.
[32] Yang J, Lee CH, Ko HJ, Suh JS, Yoon HG, Lee K, et al. Multifunctional agneto-polymeric nanohybrids for targeted detection and synergistic therapeutic effects on breast cancer. Angew Chem Int Ed Engl 2007;46:8836–9.
[33] Golzio M, Mazzolini L, Ledoux A, Paganin A, Izard M, Hellaudais L, et al. In vivo gene silencing in solid tumors by targeted electrically mediated siRNA delivery. Gene Ther 2007;14:752–9.
[34] Lee H, Lee E, Kim DK, Jang NK, Jeong YY, Jon S. Antibiofouling polymer-coated superparamagnetic iron oxide nanoparticles as potential magnetic resonance contrast agents for in vivo cancer imaging. J Am Chem Soc 2006;128:7383–9.